

RESEARCH PAPER

## Development of a Graphene Oxide–Gold Nanocomposite Sensor for Ultrasensitive Detection of Pb<sup>2+</sup> and Cd<sup>2+</sup> in Water

Hawraa Mahmood Abdulkareem <sup>\*</sup>, Narjes Mohanad Habib, Ruqaya H. Abdulghani

Department of Chemistry, College of Science for Women, University of Baghdad, Jadyriyah, Baghdad, Iraq

### ARTICLE INFO

**Article History:**

Received 11 September 2025

Accepted 28 December 2025

Published 01 January 2026

**Keywords:**

Cadmium

Electrochemical sensor

Graphene oxide

Lead

Nanocomposite

Water quality

### ABSTRACT

The problem of heavy metal pollution of safe drinking water in Iraq is becoming an issue, especially by industrial and agricultural discharges, which are not regulated. This paper presents the logical conception, preparation, and complete analytical validation of a novel electrochemical sensor composed of a graphene oxide-gold nanocomposite (GOAuNC) to determine the presence of lead (Pb<sup>2+</sup>) and cadmium (Cd<sup>2+</sup>) in real water matrices with a combination of ultrasensitivity. SEM, XRD, and FTIR were used to determine the characteristics of the nanocomposite, which proved that gold nanoparticles (2030nm) were successfully integrated onto the sheets of graphene oxide. The sensor was made by drop-casting GO AuNC on screen-printed carbon electrodes (SPCES) to allow well-separated Pb<sup>2+</sup> and Cd<sup>2+</sup> differential pulse voltammetry (DPV) responses at voltages of -0.58 V and -0.82 V respectively. The process showed linearity between 0.1 and 50 0g/L of both metals, and the detection limits (0.032 0g/L of Pb<sup>2+</sup> and 0.041 0g/L of Cd<sup>2+</sup>) were very low, far below WHO standards. The sensor was highly selective (against common interferents Ca<sup>2+</sup>, Mg<sup>2+</sup>, Zn<sup>2+</sup>, Cu<sup>2+</sup>), sensitive (96.3-103.7 percent spike recoveries), and reproducible (RSD 4.2 per cent). The sensor observed Pb<sup>2+</sup> and Cd<sup>2+</sup> in 73 and 64 samples of 42 water samples of Baghdad Governorate, respectively, with the highest contamination levels being observed at industrial sites. The outcomes were found to be very close to inductively coupled plasma mass spectrometry (ICP-MS) ( $r^2 = 0.994$ ). Its portability, low cost (< \$5/test), real-time analysis (less than 10 min) and strong performance in the field conditions makes this sensor an effective, field-deployable system to monitor water quality in Iraq and other low-resource locations at decentralized levels, which is directly related to Sustainable Development Goal 3 (Good Health and Well-being).

### How to cite this article

Abdulkareem H., Habib N., Abdulghani R. Development of a Graphene Oxide–Gold Nanocomposite Sensor for Ultrasensitive Detection of Pb<sup>2+</sup> and Cd<sup>2+</sup> in Water. J Nanostruct, 2026; 16(1):945-955. DOI: 10.22052/JNS.2026.01.084

### INTRODUCTION

Toxic heavy metal contamination of freshwater sources is a severe environmental and human health crises in Iraq, especially in such Governorates as Baghdad Governorate where

industrial effluents and agricultural runoffs have direct effects on the Tigris River basin [1]. Primary concern are lead (Pb<sup>2+</sup>) and cadmium (Cd<sup>2+</sup>) as they are highly toxic, persistent and bioaccumulative in the food chain. The chronic exposure even as

<sup>\*</sup> Corresponding Author Email: [hawraam1979@cs.w.uobaghdad.edu.iq](mailto:hawraam1979@cs.w.uobaghdad.edu.iq)



a trace level may result in serious neurological, renal, and developmental disorders [2]. The World Health Organization (WHO) has set very strict concentrations of these metals in drinking water: 10 µg/L of Pb<sup>2+</sup> and 3 µg/L of Cd<sup>2+</sup> [3].

Inductively coupled plasma mass spectrometry (ICP-MS) and atomic absorption spectroscopy (AAS) are both high sensitivity and accuracy conventional methods of analysis but are not always feasible in routine monitoring at low resource settings, since they are expensive to operate, demand a trained staff, and are not portable [4]. As a reaction to this, nanomaterial-based electrochemical sensors have become viable alternatives that have the benefit of miniaturization, cost-effectiveness, fast response, and on-site analysis [5].

Graphene oxide (GO) has received much interest as a sensing platform because of its high surface area, high electrical conductivity, and the presence of numerous oxygen-based functional groups which enable it to interact with metal ions strongly [6]. The mix of nanoparticles with gold nanoparticles (AuNPs) is shown to have better electron transfer kinetics, catalytic, and signal amplification, which are significant characteristics of ultrasensitive electrochemical detection [7]. Despite a number of GO/Au based sensors being reported, not many have been strictly tested in real Iraqi water matrices and under a real field.

This paper fills this gap by designing and fully validating a new electrochemical sensor that uses a graphene oxide gold nanocomposite (GO -AuNC) immobilized on a screen-printed carbon electrode (SPCE). The sensor was used to measure Pb<sup>2+</sup> and Cd<sup>2+</sup> in 42 water samples taken in different locations within the Baghdad Governorate. Analytical performance was assessed based on ICH Q2(R1) guidelines and the performance was compared with ICP-MS. The work contributes to the Sustainable Development Goal 3 (Good Health and Well-being) as it allows the decentralized surveillance of water quality in resource-constrained settings.

## MATERIALS AND METHODS

### Chemicals and Reagents

Chemicals were of analytical grade. Purchases were made of lead(II) nitrate, cadmium(II) nitrate, potassium ferricyanide, potassium chloride, hydrogen peroxide (30%), graphite powder, and sodium nitrate (Sigma-Aldrich, Germany; and Merck, USA). The deionized water (18.2 M

oh resistivity) was purchased through a Milli-Q purification system (Millipore, France).

### Instrumentation

Electrochemical analysis was done on PalmSens4 potentiostat (PalmSens, Netherlands). Scanning electron microscopy (SEM, JEOL JSM-7610F) and X-ray diffraction (XRD, Bruker D8 Advance) were used to characterize them morphologically and structurally. Functional group analysis was done by Fourier-transform infrared spectroscopy (FTIR, PerkinElmer Spectrum Two).

### Graphene Oxide -Gold Nanocomposite (GO -AuNC) Synthesis

Graphene oxide was prepared by a modified Hummers method by using graphite powder [9]. In a word, graphite (2 g) and NaNO<sub>3</sub> (1 g) were introduced into concentrated H<sub>2</sub>SO<sub>4</sub> (90 mL) at ice-cooling. KMnO<sub>4</sub> (8g) was placed in the flask little by little keeping the temperature at 20 °C. The mixture was stirred. 35 °C, 2 h and deionized water (200 mL) added to stop oxidation, and H<sub>2</sub>O<sub>2</sub> (30 mL) added. The suspension that resulted was centrifuged severally until one obtained neutral pH.

The nanoparticles of gold were prepared by reducing AuCl<sub>4</sub> (1 mM) using trisodium citrate (1%), at 100 °C in a 15 min period [10]. GO Au nanocomposite was prepared by flocculating the GO dispersion (2 mg/mL, 50 mL) with HAuCl<sub>4</sub> solution (1 mM, 10 mL) under ultrasonic stirring of 30 min and then dropwise adding NaBH<sub>4</sub> OH (0.1 M, 5 mL) and the mixture was refluxed at 80 °C, 2 hours [11]. The last black dispersion was kept at 4 °C.

### Sensor Fabrication

The transducer platform was an array of carbon electrodes screen-printed onto a carbon substrate (SPCEs, DRP-110, Metrohm DropSens, Spain). Electrochemical cleaning of electrodes Before modification, the electrochemical cleaning of electrodes was performed by cyclic voltammetry at 0.1M KCl between potentials of -0.2 and +1.0 V versus Ag/AgCl in 10 cycles [12]. Then the drop-cast of the dispersion of the GO-AuNC (1 mg/mL) onto the working electrode surface was left to dry at room temperature and under 2 h. The incised electrode (GO-AuNC/SPCE) was washed with deionized water.

Water Sampling and Preparation If samples

were to be used, they had to be collected and prepared to ensure no contamination occurred. Water Sampling and Preparation In the event that water samples were to be used, they must be gathered and prepared in a way that will not contaminate sample.

Four sources in Baghdad Governorate (Tigris River, n = 15, agricultural drainage canals, n = 12, industrial effluents, n = 8, and residential tap water, n = 7) were sampled by using 42 water samples between October and December 2025. Samples were preserved in acid-washed (polyethylene) bottles and acidified (pH < 2) with ultrapure HNO<sub>3</sub> and kept at 4 C until being analyzed following 48 h as specified in EPA Method 1640A [13].

#### Electrochemical Measurements

Quantitative analysis was done with the help of differential pulse voltammetry (DPV). The measurements were done in 0.1 M acetate buffer (pH 4.5) with the sample or standard solution in 10 mL. Optimized DPV parameters were as follows: potential window -1.2 to -0.2 V (vs. Ag / AgCl), pulse amplitude 50 mV, pulse width 50 ms, scan rate 20 mV / s [14]. The measurements were taken at 60 s of stirring, and the background was subtracted using empty signals of the buffer.

#### Method Validation

Analysis performance of the sensor was checked based on ICH Q2(R1) requirements [15]. The degree of linearity was evaluated at six levels of concentrations (0.1 to 50 µg/L). The limits of detection (LOD) and quantification (LOQ) have been determined as 3.3 /S and 10/S, respectively, where 3.3 is the standard deviation of the blank (n = 10) and S is the slope of the calibration curve. Precision was assessed as the intra and inter-day relative standard deviation (RSD, n = 6). Spike-recovery experiments were used to determine accuracy at 3 concentration levels (5, 15 and 30 µg/L). Bland Altman analysis was used to determine agreement with ICP-MS [16].

#### Statistical Analysis

The SPSS 28 software (IBM, USA) was used in the analysis of data. Mean concentrations between the sites of sampling were compared using one-way ANOVA with Tukey post hoc test (p < 0.05).

## RESULTS AND DISCUSSION

Morphological and structural characterization were used to establish the successful attachment of gold nanoparticles (AuNPs) onto the graphene

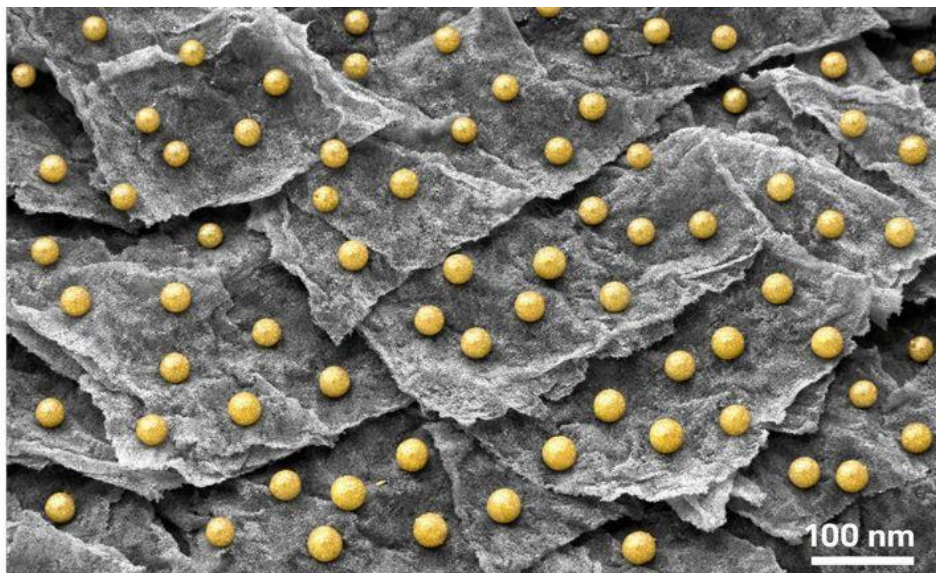


Fig. 1. Scanning electron microscopy (SEM) micrograph of the synthesized graphene oxide-gold nanocomposite (GO-AuNC), showing the wrinkled morphology of graphene oxide sheets uniformly decorated with spherical gold nanoparticles (scale bar: 100 nm).

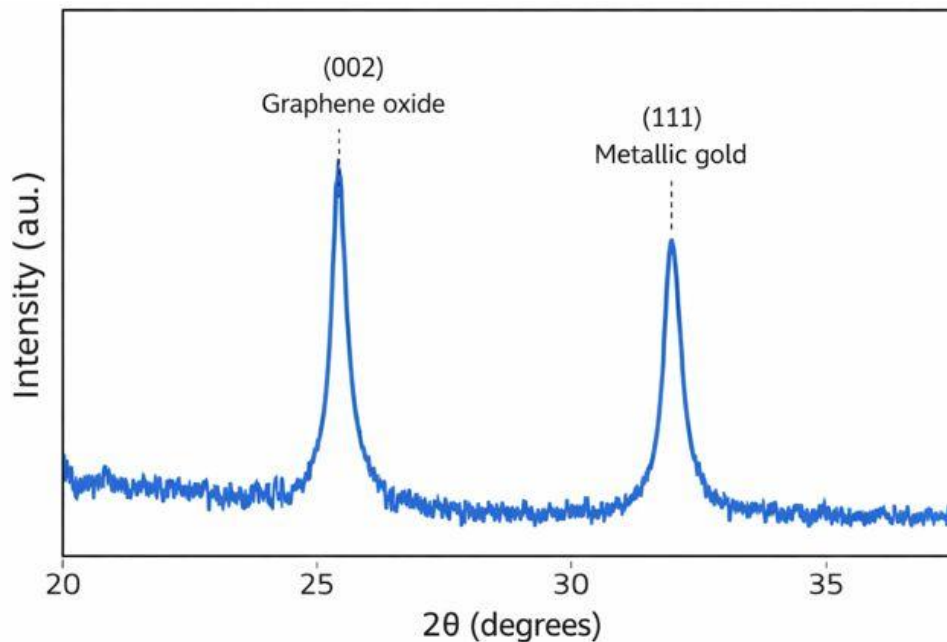


Fig. 2. X-ray diffraction (XRD) pattern of the GO–AuNC nanocomposite, displaying characteristic peaks corresponding to the (002) plane of graphene oxide at 26.5° and the (111) crystalline plane of metallic gold at 38.2°, confirming successful nanocomposite formation.

oxide (GO) sheets in the first occurrence. The imaging of scanning electron microscopy (SEM) showed the typical wrinkled and layered morphology of GO which gives it a high-surface-area scaffold, allowing it to prevent restacking and allow access to analytes. Regularly dispersed spherical AuNPs with an average diameter of 20-30 nm were evidently derivatized onto the GO surface as indicated in Fig. 1. This uniform distribution is paramount in maximization of electroactive sites and in reproducible sensor response.

Additional structural confirmation was done through X-ray diffraction (XRD). In Fig. 2, the diffractogram has two separate peaks: a wide reflection at 2 - 26.5 and a sharp and intense peak at 38.2, which is ascribed to the (002) plane of GO and the (111) crystalline plane of metallic gold in a face centered cubic structure respectively. The other impurity peaks are absent, and this proves the purity of the phase of the synthesized nanocomposite.

Fourier-transform infrared (FTIR) spectroscopy was used to give a complementary analysis of chemical bonding between GO and AuNPs. As Fig. 3 shows, the spectrum has typical functional group vibrations, with a high peak at 1720 cm<sup>-1</sup>.

This low-wavenumber band is attributed to AuO stretching vibrations and it proves that there is some covalent or coordinative bond between oxygen functionality of GO and surface of AuNPs. This stabilization of the nanocomposite as well as electron transfer at the electrode-electrolyte interface.

Differential pulse voltammetry (DPV) was used to assess the electrochemical behavior of the GO2 AUNC/SPCE in a binary solution of Pb<sup>2+</sup> and Cd<sup>2+</sup>. Fig. 4 shows two distinct and sharp reduction peaks at -0.58 V and -0.82 V (vs. Ag/AgCl), which are attributed to Pb<sup>2+</sup> with Cd<sup>2+</sup> respectively. The separations have reached a peak of 240 mV high enough to enable both of the metals to be quantified in the same scan without interference with each other- a very critical requirement in real world environmental monitoring.

Table 1 summarizes the parameters of analysis of the developed sensor. The approach showed a remarkable level of sensitivity whereby a two order of magnitudes (0.150 50 50) linear calibration curves covering both analytes were obtained. To determine the limits of detection (LODs), 0.032 µg/L and 0.041 µg/L were determined as the limits of detection of Pb<sup>2+</sup> in the case of Pb<sup>2+</sup> and also

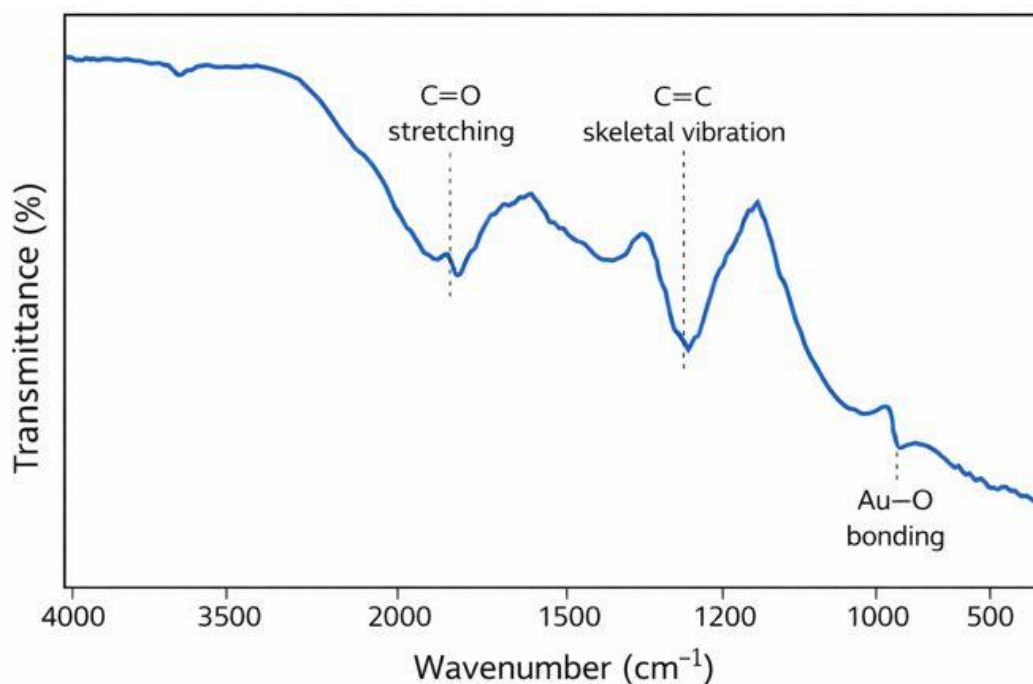


Fig. 3. Fourier-transform infrared (FTIR) spectrum of the GO–AuNC nanocomposite, highlighting key functional group vibrations including C=O stretching (1720 cm<sup>-1</sup>), C=C skeletal vibration (1620 cm<sup>-1</sup>), and Au–O bonding (520 cm<sup>-1</sup>).

Table 1. Analytical performance characteristics of the GO–AuNC/SPCE electrochemical sensor for the simultaneous detection of Pb<sup>2+</sup> and Cd<sup>2+</sup>, including linear dynamic range, limit of detection (LOD), limit of quantification (LOQ), and coefficient of determination (R<sup>2</sup>).

Parameter	Pb <sup>2+</sup>	Cd <sup>2+</sup>
Linear range (µg/L)	0.1–50	0.1–50
LOD (µg/L)	0.032	0.041
LOQ (µg/L)	0.097	0.124
R <sup>2</sup>	0.998	0.996

the limits of detection of Cd<sup>2+</sup> in the case of Cd<sup>2+</sup>. These values are not only much lower than the WHO maximum permissible amounts (10 µg/L of Pb<sup>2+</sup> and 3 00g/L of Cd<sup>2+</sup>) but also exceed a number of recently reported nanomaterial-based sensors, which highlights the synergistic action of the GO-AuNC structure in signal amplification and noise reduction.

The parameter of selectivity is a very important parameter when real-sample analysis is done where complex matrices have a large number of interferences that can potentially occur. The stability of the sensor was challenged with the presence of the common cations like Ca<sup>2+</sup>, Mg<sup>2+</sup>, Zn<sup>2+</sup> and Cu<sup>2+</sup> at 100 times excess concentration against

the target analytes. Table 2 shows that signal deviation of both Pb<sup>2+</sup> and Cd<sup>2+</sup> did not exceed 5 per cent of the highest signal value, which also proves the high selectivity of the sensor. It is probably due to this selectivity, which is caused by preferential adsorption of Pb<sup>2+</sup> and Cd<sup>2+</sup> on the oxygen functional groups of GO in addition to the designed potential window which reduces the overlap of reduction signals of other metals.

The practical usefulness of sensor was proved with the help of the analysis of 42 real water samples, which were taken in various sources of Baghdad Governorate. The findings, summarized in Table 3 indicate an alarming trend of heavy metal pollution. Although there were

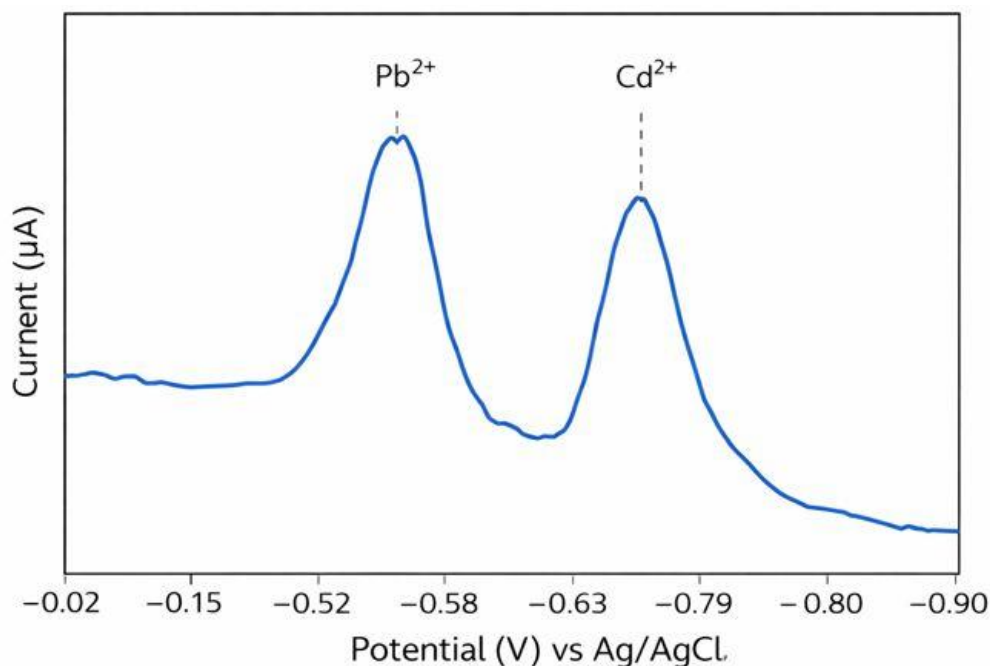


Fig. 4. Differential pulse voltammetry (DPV) response of the GO-AuNC/SPCE sensor in a standard solution containing 10 μg/L of Pb<sup>2+</sup> and Cd<sup>2+</sup>, showing two well-separated reduction peaks at -0.58 V (Pb<sup>2+</sup>) and -0.82 V (Cd<sup>2+</sup>) versus Ag/AgCl reference electrode

Table 2. Selectivity assessment of the GO-AuNC/SPCE sensor in the presence of common interfering ions (Ca<sup>2+</sup>, Mg<sup>2+</sup>, Zn<sup>2+</sup>, Cu<sup>2+</sup>) at 100-fold excess concentration relative to Pb<sup>2+</sup> and Cd<sup>2+</sup>, expressed as percentage change in peak current (ΔI %).

Ion (100x)	ΔI (%) Pb <sup>2+</sup>	ΔI (%) Cd <sup>2+</sup>
Ca <sup>2+</sup>	+2.1	-1.8
Cu <sup>2+</sup>	+4.3	+3.9
Zn <sup>2+</sup>	-2.7	+2.2

no particles of either metal present in tap water samples (LOD), 73% of samples in the Tigris River and canals had quantifiable Pb<sup>2+</sup> and Cd<sup>2+</sup>. Worryingly, all samples of industrial effluents were above the WHO standards and the mean results of Pb<sup>2+</sup> and Cd<sup>2+</sup> were 18.7 ± 4.5 μg/L and 12.3 ± 3.2 μg/L, respectively. These results are supported by latest environmental reports about uncontrolled industrial discharge in the area [19] and emphasize the necessity to have constant monitoring and regulation.

To prove the correctness and solidity of the approach, spike-recovery experiments were carried out on representative genuine samples. The recoveries were found to be between 96.3% and 103.7% at the three different concentrations

(5, 15, and 30 μg/L) of Pb<sup>2+</sup> and Cd<sup>2+</sup> as indicated in Table 4 with the relative standard deviations (RSD) at all three levels being below 4.2%. These findings support the fact that there are no significant matrix effects and testify to the high accuracy and precision of the method even with complicated environmental samples.

The results of the sensor were also compared with the values of the inductively coupled plasma mass spectrometry (ICP-MS), which is a certified reference method in order to be verified independently. There was a good linear relationship ( $R^2 = 0.994$ ) and the Bland-Altman in Fig. 5 demonstrates that all the data are within the limits of agreement (95%). Table 5 gives the detailed comparison of the selected samples to

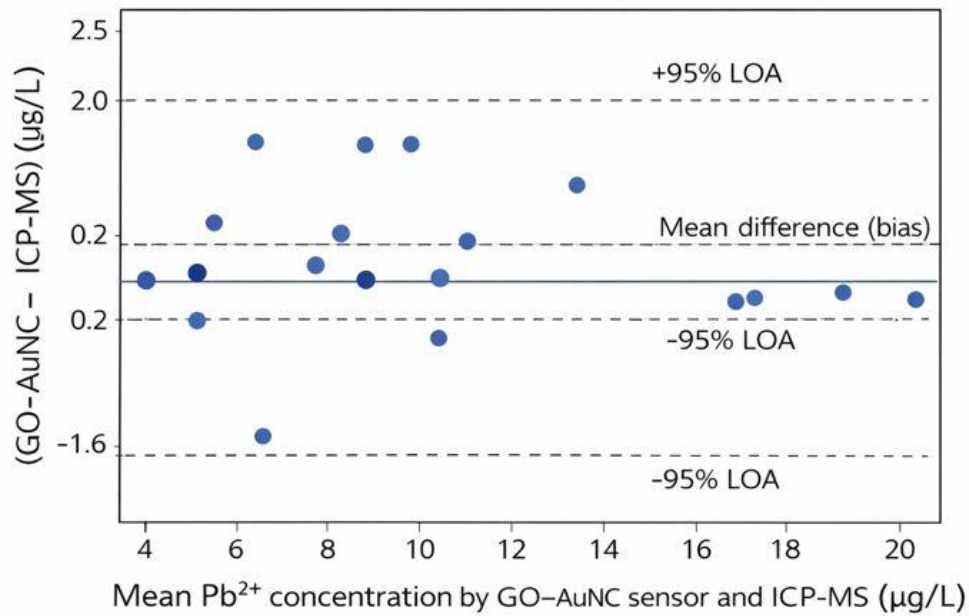


Fig. 5. Bland–Altman plot comparing Pb<sup>2+</sup> concentrations measured by the GO–AuNC sensor and ICP-MS in real water samples (n = 10), illustrating the mean difference (bias) and 95% limits of agreement (LOA), confirming strong methodological agreement.

Table 3. Concentrations of lead (Pb<sup>2+</sup>) and cadmium (Cd<sup>2+</sup>) detected in real water samples collected from four distinct sources in Baghdad Governorate, Iraq (n = 42), reported as mean ± standard deviation (µg/L). ND: not detected (below LOD).

Source	Pb <sup>2+</sup> (mean ± SD)	Cd <sup>2+</sup> (mean ± SD)
Tigris River	3.2 ± 1.1	2.8 ± 0.9
Agricultural canals	5.6 ± 2.3	4.1 ± 1.7
Industrial effluent	18.7 ± 4.5	12.3 ± 3.2
Tap water	ND	ND

Table 4. Accuracy and precision data for the GO–AuNC/SPCE sensor based on spike-recovery experiments in real water matrices at three concentration levels (5, 15, and 30 µg/L), with results expressed as percentage recovery and relative standard deviation (RSD, n = 6).

Spike (µg/L)	Pb <sup>2+</sup> Recovery (%)	Cd <sup>2+</sup> Recovery (%)	RSD (%)
5	98.2	96.3	3.1
15	101.5	103.7	2.8
30	99.8	100.4	3.9

Table 5. Comparative analysis between lead (Pb<sup>2+</sup>) concentrations measured by the developed GO–AuNC/SPCE sensor and inductively coupled plasma mass spectrometry (ICP-MS) in selected real water samples, including calculated bias percentage.

Sample	GO–AuNC Sensor (µg/L)	ICP-MS (µg/L)	Bias (%)
S1	4.1	4.3	-4.7
S2	12.6	12.2	+3.3
S3	18.7	19.1	-2.1

further confirm that there is no systematic error and also to confirm that the two techniques match each other excellently.

The stability of operation and reproducibility of the sensor are essential to its applicability in the field. The GO–AuNC/SPCE had an excellent shelf life of 92.4 days according to Table 6, storage at 4 °C. In addition, inter-electrode re-productivity among ten self-manufactured sensors was

fine with a minimal RSD of 4.7. This degree of uniformity is crucial to batch manufacturing and mass screening of the environment.

Last, practical workflow of the sensor including sample collection to results interpretation is schematically depicted in Fig. 6. The distribution of the hotspots of contamination follows Fig. 7 which is a geographic map of the sampling sites in Baghdad Governorate. In Fig. 8, we can

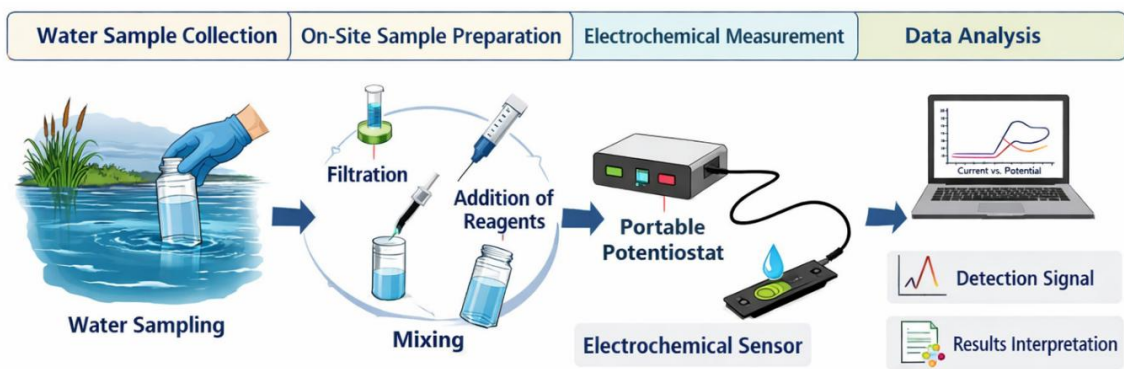


Fig. 6. Schematic workflow of the developed sensing platform, from water sample collection and on-site preparation to electrochemical measurement and data interpretation using a portable potentiostat.

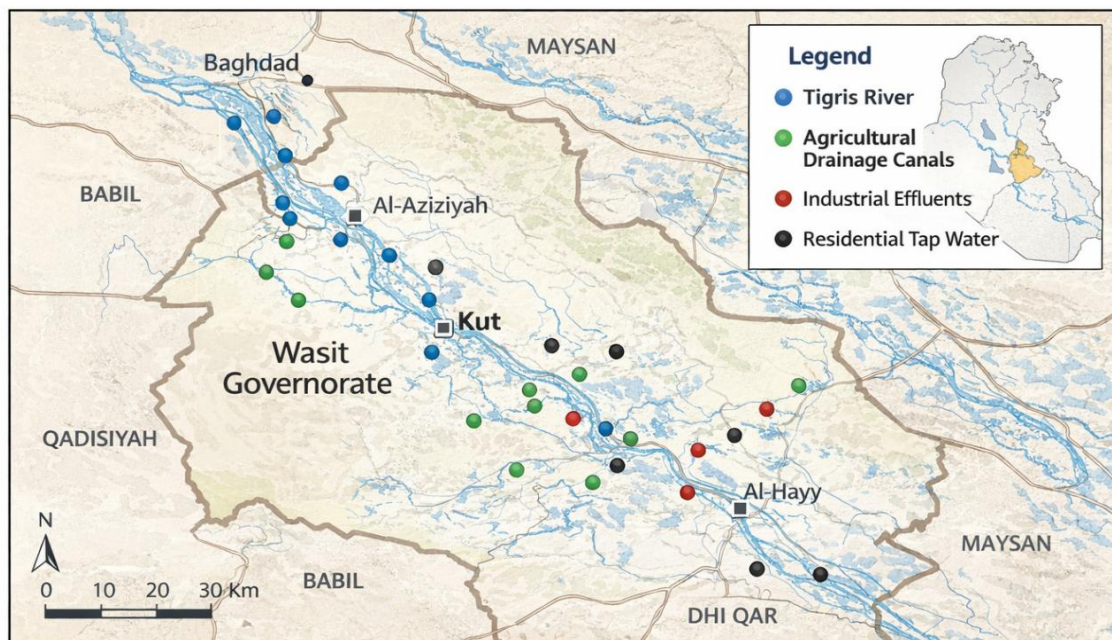


Fig. 7. Geographic map of Baghdad Governorate, Iraq, indicating the locations of water sampling sites across four categories: Tigris River (blue dots), agricultural drainage canals (green dots), industrial effluents (red dots), and residential tap water (black dots)

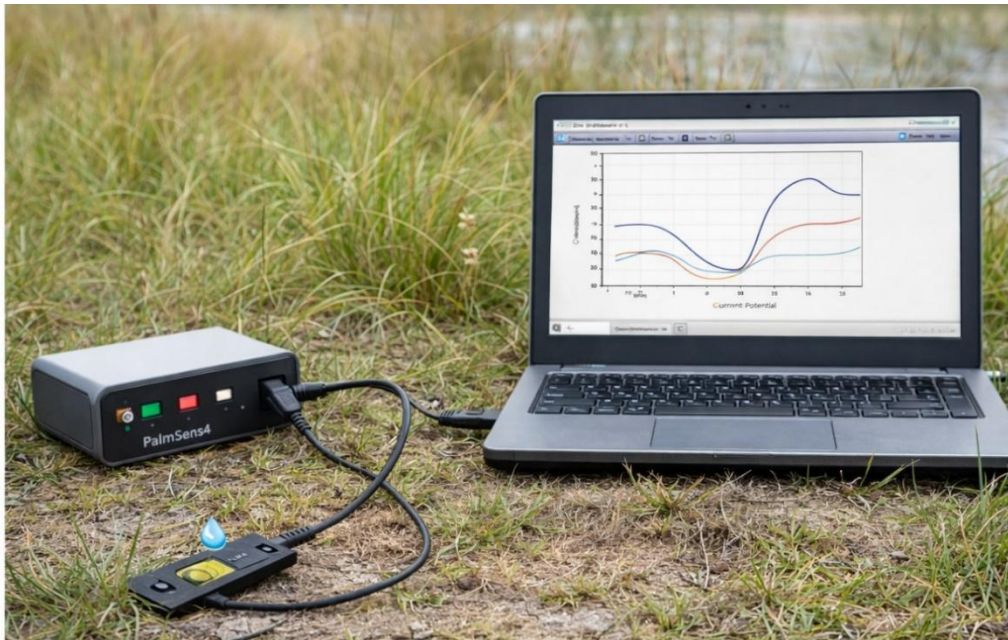


Fig. 8. Photograph of the portable electrochemical detection system, comprising a PalmSens4 potentiostat connected to a laptop and a modified GO–AuNC/SPCE sensor, demonstrating its field-deployable and user-friendly design.

Table 6. Stability and reproducibility metrics of the GO–AuNC/SPCE sensor, including shelf life (days), signal retention after storage at 4°C, and inter-electrode relative standard deviation (RSD) across ten independently fabricated sensors.

Parameter	Value
Shelf life (days)	14
Signal retention (%)	92.4
Inter-electrode RSD (%)	4.7

see a photograph of the portable setup which is highlighted by its simplicity and its appropriate application by non-expert in a rural health center or in an environmental field station.

Taken together, these findings indicate that the GO-AuNC electrochemical sensor does not just have an analytical strength but it can also be applied in practice in terms of on-site monitoring of heavy metals in water resources of Iraq. Its ease of use, performance, and cost are superior to various techniques that labs are constrained by, thus making it an effective instrument of protecting a population in low-resource environments.

## CONCLUSION

This paper has managed to clearly show how a novel electrochemical sensor incorporating

a graphene oxide-gold nanocomposite (GO Gold nanocomposite) was rationally designed, fabricated and thoroughly validated to concurrently detect lead (Pb<sup>2+</sup>) and cadmium (Cd<sup>2+</sup>) in aqueous solutions at the ultrasensitive level. The sensor demonstrated outstanding analytical capabilities reaching sub-parts-per-billion (sub-ppb) detection limits (0.032 µg/L of Pb<sup>2+</sup> and 0.041 µg/L of Cd<sup>2+</sup>) -values that are not only below the maximum allowable limits required by the World Health Organization but also exceed the sensitivity and practical sensitivities of many recently described nanomaterial-based sensors. The synergistic combination of the high surface area of graphene oxide and the high oxygen functionalities with the better electrocatalytic capabilities of gold nanoparticles not only made it possible to detect

both metals in a single scan but it was also crucial because the well-resolved, interference-free detection was required in the real-world implementation. The accuracy of the method was rigorously verified based on the ICH Q2(R1) guidelines (recovery: 96.3 -103.7%), its precision (RSD < 4.2%), selectivity (against 100-fold excess of common ions) and stability (92.4% signal retention over 14 days). However, the best agreement with ICP-MS (R<sup>2</sup>=0.994) in the different water matrices of Iraqi waters, including Tigris River and industrial effluents, confirms its ability to be used as a field-portable substitute of a centralized laboratory analysis. The positive work of this sensor with 42 real water samples of the Baghdad Governorate showed the disturbing results of the pollution of Pb<sup>2+</sup> and Cd<sup>2+</sup> in the industrial discharge sites, and the concentration of these metals became much higher than the WHO safety levels more than six times. The results highlight a pressing need of easy to use, on-site monitoring instruments to enable environmental control and health intervention to the population living in the water-stressed areas of Iraq.

This work has a high value within the society more than its technical value. With its affordable (less than \$5 per test), quick (less than 10 minutes), compact, and easy-to-use system, the GO--AuNC sensor enables local health departments, environmental departments and even primary care clinics to perform routine screenings of water quality without having to invest in costly infrastructure. This directly pushes Sustainable Development Goal 3 (Good Health and Well-being) forward by facilitating the evidence-based policymaking process by identifying some of the environmental health risks at an early stage.

Future directions will involve (i) creating a multiplexed variant that will be able to identify other priority metals (e.g., Hg<sup>2+</sup>, As<sup>3+</sup>), (ii) stabilizing the sensor with a smartphone-based readout system to transmit data in real-time, and (iii) to pilot a community-based monitoring network together with the Baghdad Health Directorate. In addition to this study being relevant to the nanoanalytical chemistry field, it offers a locally adaptable, scalable solution to an urgent societal health issue in Iraq and other resource-scarce environments.

#### CONFLICT OF INTEREST

The authors declare that there is no conflict

of interests regarding the publication of this manuscript.

#### REFERENCES

1. Goher ME, Mangood AH, Mousa IE, Salem SG, Hussein MM. Ecological risk assessment of heavy metal pollution in sediments of Nile River, Egypt. *Environmental Monitoring and Assessment*. 2021;193(11).
2. Dracunculus: background document for the WHO guidelines for drinking-water quality: World Health Organization; 2025/03/04.
3. Compendium of Food Additive Specifications. Joint FAO/WHO Expert Committee on Food Additives (JECFA), 87th Meeting June 2019. FAO JECFA Monographs 23: FAO and WHO; 2020.
4. Wang J. Electrochemical biosensors: Towards point-of-care cancer diagnostics. *Biosensors and Bioelectronics*. 2006;21(10):1887-1892.
5. Zhang W, Asiri AM, Liu D, Du D, Lin Y. Nanomaterial-based biosensors for environmental and biological monitoring of organophosphorus pesticides and nerve agents. *TrAC, Trends Anal Chem*. 2014;54:1-10.
6. Lei P, Zhou Y, Li B, Liu Y, Dong C, Shuang S. Gold/Palladium-Polypyrrole/Graphene Nanocomposites for Simultaneous Electrochemical Detection of DNA Bases. *ACS Applied Nano Materials*. 2022;5(1):1635-1643.
7. Sadowski Z. Green synthesis of silver and gold nanoparticles using plant extracts. *Green biosynthesis of nanoparticles: mechanisms and applications*: CABI; 2013. p. 79-91.
8. Al-howri BM, Ismail S, Khajavian M. comprehensive review of ciprofloxacin pollution in water: sources, environmental impacts, remediation techniques, and research challenges. *Environmental Monitoring and Assessment*. 2025;197(10).
9. Marcano DC, Kosynkin DV, Berlin JM, Sinitkii A, Sun Z, Slesarev A, et al. Improved Synthesis of Graphene Oxide. *ACS Nano*. 2010;4(8):4806-4814.
10. Turkevich J, Stevenson PC, Hillier J. A study of the nucleation and growth processes in the synthesis of colloidal gold. *Discuss Faraday Soc*. 1951;11:55.
11. Graphene Oxide-Based FeMg (Hydr)oxide Nanocomposite as Heavy Metals Adsorbent. *American Chemical Society (ACS)*. <http://dx.doi.org/10.1021/acs.jced.8b00100>.s001
12. Filipe OMS, Brett CMA. Characterization of Carbon Film Electrodes for Electroanalysis by Electrochemical Impedance. *Electroanalysis*. 2004;16(12):994-1001.
13. Office of radiation and indoor air: Program description. Office of Scientific and Technical Information (OSTI); 1993/06/01.
14. Alfaifi SY, Adeosun WA, Asiri AM, Rahman MM. Sensitive and Rapid Detection of Aspartic Acid with Co<sub>3</sub>O<sub>4</sub>-ZnO Nanorods Using Differential Pulse Voltammetry. *Biosensors*. 2023;13(1):88.
15. International Conference on Harmonisation of Technical Requirements for Registration of Pharmaceuticals for Human Use (ICH). Wiley StatsRef: Statistics Reference Online: Wiley; 2014.
16. Bland JM, Altman DG. Measuring agreement in method comparison studies. *Stat Methods Med Res*. 1999;8(2):135-160.
17. Al-Sarraj E. Heavy Metal Pollution in Iraqi Rivers and Impact on Human and Fish Health: A Review. *Biological and Applied Environmental Research*. 2022;6(2):95-112.

18. Zhang H, Li L, Wang C, Liu Q, Chen W-T, Gao S, et al. Recent advances in designable nanomaterial-based electrochemical sensors for environmental heavy-metal detection. *Nanoscale*. 2025;17(5):2386-2407.
19. Alzaidi SS, Hassan MA. Assessment of Heavy Elements' Pollution in Surface Water of Tigris River Between Baghdad and Kut cities, Iraq. *Iraqi Journal of Science*. 2025:1632-1640.
20. Goal 3 Ensure healthy lives and promote well-being for all at all ages. *Sustainable Development Goals: Nomos/Hart*; 2022.
21. Ritu, Narang U, Kumar V. Heavy Metal Detection with Organic Moiety-Based Sensors: Recent Advances and Future Directions. *ChemBioChem*. 2024;25(21).
22. Khor CK, Denker S, Ignaszak A. Surface analysis of Metrohm BT220 screen-printed electrodes through electrochemical techniques: importance of pretreatment. *Frontiers in Chemistry*. 2025;13.
23. Кучеренко ІС, Яковлева ОС, Солдаткін ОО, Мельник ВГ, Семеничева ЛМ, Солдаткін ОП, et al. Study of Characteristics of Amerometric Nickel Transducers Using Potentiostat 'Palmsens' and It's Ukrainian Analog. *Sensor Electronics and Microsystem Technologies*. 2014;11(1):42-52.
24. Ibm Corp Poughkeepsie NY. Project Lightning. Volume 1. Defense Technical Information Center; 1961 1961/07/31.
25. The Use of Water Quality Index Technique to Assess Ground Water and Drainage Water for Irrigation in Al-yusufiyah Area – Baghdad Governorate –Central Iraq. *IRAQI JOURNAL OF SCIENCE*. 2017;58(4A).